ISSN 8755-6839

SCIENCE OF **TSUNAMI HAZARDS**

Journal of Tsunami Society International

Volume 35 **Number 3** **2016**

FEATURES AND PROBLEMS WITH HISTORICAL GREAT EARTHQUAKES AND TSUNAMIS IN THE MEDITERRANEAN SEA

[1] Lobkovsky L., [2] Mazova R., [2] Tyuntyaev S.,[2] Remizov I..

[1]P.P. Shirshov Institute of Oceanology, Russian Academy of Sciences, Moscow, Russia
[2]R.E.Alekseev Nizhny Novgorod State Technical University, Nizhny Novgorod, Russia

E-mail address:
llobkovsky@ocean.ru; raissamazova@yandex.ru; ser.tyuntyaev@gmail.com i.v.remizov@yandex.ru

ABSTRACT

The present study examines the historical earthquakes and tsunamis of 21 July 365 and of 9 February 1948 in the Eastern Mediterranean Sea. Numerical simulations were performed for the tsunamis generated by underwater seismic sources in frames of the keyboard model, as well as for their propagation in the Mediterranean Sea basin. Similarly examined were three different types of seismic sources at the same localization near the Island of Crete for the earthquake of 21 July 365, and of two different types of seismic sources for the earthquake of 9 February 1948 near the Island of Karpathos. For each scenario, the tsunami wave field characteristics from the earthquake source to coastal zones in Mediterranean Sea's basin were obtained and histograms were constructed showing the distribution of maximum tsunami wave heights, along a 5-m isobath. Comparison of tsunami wave characteristics for all the above mentioned scenarios, demonstrates that underwater earthquakes with magnitude M > 7 in the Eastern Mediterranean Sea basin, can generate waves with coastal runup up to 9 m.

KEYWORDS: Mediterranean Region, Great Historical Tsunamigenic Earthquakes, Seismic Source, Tsunami Generation, Tsunami Propagation, And Numerical Simulation

1. INTRODUCTION

The Mediterranean Sea region is characterized by high seismicity. The historical record indicates that potentially destructive tsunamis are possible and need to be further studied. The Eastern Mediterranean basin is particularly the most active (Pararas-Carayanis, 2001; Tinti et al, 2005; Papadopoulos et al., 2010). The eastern basin has significant sediment layers, which can reach up to 5-8 km in thickness (Papadopoulos et al., 2010)). Also, it has seismic arcs which are characteristic of transform zones – such as the Ionian Island Arc and the western and southern Crete Arc which extends to the Island of Rhodes, as well as deep sea trenches, such as the Hellenic deep sea trench with a depth of up to 5 km. The Hellenic Seismic Arc is one of the best known geological features of the Eastern Mediterranean and includes a deep-sea trench (Fig.1, red line) in its convex side (Hellenic trench), and an arc of underwater sediments, as well as a volcanic arc and a marginal sea (the Aegean Sea) in its concave side (Pararas-Carayanis, 2001; 2005; Papadopoulos et al., 2010).

Figure 1. Scheme of faults (red lines) in Mediterranean region.
The yellow arrows indicate direction of continental plate motion ((see, (EC, 2016)).

The seismic activity is high at shallow and moderate depths, and earthquakes that can reach magnitude of the order of M ~ 8 are possible. The motions of the continental plates (Fig.1) lead to an increase of stress in fault regions. Such interactions increase the potential of high tsunamicity, which gradually increases from the west to the east within the Mediterranean basin, particularly in the vicinity of Greece and the surrounding regions (Papazachos, B. C. 1996; Pararas-Carayanis, 2001; Papadopoulos et al., 2010; Pararas-Carayannis, Mader, 2011, EC, 2016).

Several significant earthquakes have occurred in regions of the Eastern Mediterranean Sea which generated local or regional destructive tsunamis in the past. Based on numerous historical documents, a great earthquake on 21 July 365 A.D. generated a devastating tsunami - now considered as the most catastrophic event in the Mediterranean Sea (Pararas-Carayanis, 2001; Tinti et al, 2005; Salamon et al., 2007; Shaw et al., 2008; Papadopoulos et al., 2010; Yolsal-Çevikbilen, Taymaz, 2012. Then, in February of 1948, another destructive tsunami struck the coasts of Karpathos Island. The main cause of such tsunamigenic earthquakes, results from the partial breaking of the African plate and its collision with the Eurasian plate (see Fig.1).

2. STATEMENT OF THE PROBLEM

2.1. Formation of tsunami source

Great earthquakes occur in zones of great faults in the Mediterranean basin, as shown in Fig.1. Many of the great underwater shallow earthquakes generate destructive tsunami. The tsunami generation mechanisms, the initial velocity and propagation of the waves and the terminal characteristics of inundation at a given coast (particularly in near-field zone) depend directly on the dynamic processes at the earthquake source (Lobkovsky, 1988; Lobkovsky et al., 2006). The present study describes the seismic processes of the earthquake source and the keyboard modelling of tsunamigenic earthquakes, where the vertical displacement of crustal blocks, is applied to determine the above listed parameters. (Lobkovsky, 1988)). The initial stress distribution in the seismic source essentially determines the character of crustal motions that generate a tsunami. The selection of a model for the seismic source is first of all determined by the spatial and temporal scales of corresponding wave motions in the basin (Lobkovsky, 1988; Lobkovsky et al., 2006). The present study addresses the numerical simulation of two historic catastrophic earthquakes in the Eastern Mediterranean: the earthquake of 21 July 365 A.D with possible magnitude M = 8.2 near the western the Island of Karpathos in the Aegean Sea.

Since the mechanisms of the seismic sources of both earthquakes are unknown, then, by taking the source mechanism from tectonic relationships (Lobkovsky et al., 2006)) and by using empirical formulas correlating earthquake magnitudes and displacement values along faults (Wells, Coppersmith, 1994), it is possible to compute approximately the size of the seismic source and the vertical components of seafloor displacement at the source. The estimate for the 365 A.D earthquake with a magnitude 8.2, had a source of 190 km in length and a width of nearly 40 km, while maximum displacement value is 9 m. For the 1948 tsunamigenic earthquake with magnitude M = 7.5, the source is 26 km in length, 26 km in width and with the crustal displacement estimated at 5 m.

For the 365 A.D. earthquake, three possible scenarios of were considered of crustal motions at the seismic source along the fault zone near the western region of the Island of Crete. (Figs. 2-4), (cf. with (Pararas-Carayanis, Mader, 2011))

SCENARIO 1: The seismic source being a single block, which can be moved up and down for given value with different velocities – the location of seismic source for this scenario is illustrated in Fig. 2 a,b.

SCENARIO 2: A two-block source divided along its length in two equal-in-width blocks, one of which is oriented to the Island of Crete (block 1) moving down, and a block 2 which begins to move up after the first block motion stops; the location of the seismic source for scenario 2 is illustrated in Fig. 3a, b.

SCENARIO 3: For the third scenario, the kinematic model of three-block keyboard source is considered, in which the source blocks move successively to different distance up and down at different times. The location of the seismic source for scenario 3 is presented in Fig.4 a,b.

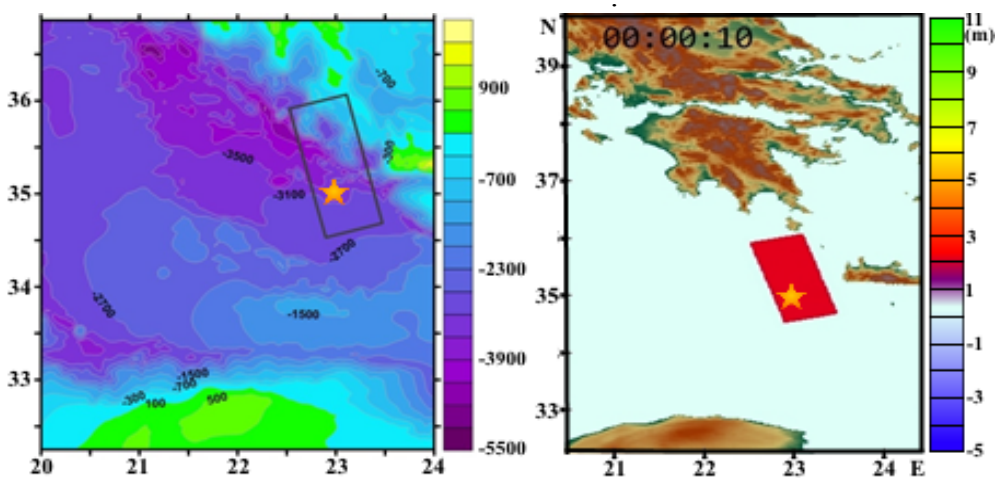

а) б)

Figure 2. Location of seismic source at earthquake of 365, SCENARIO 1
a) bathymetric map; b) topographic map.

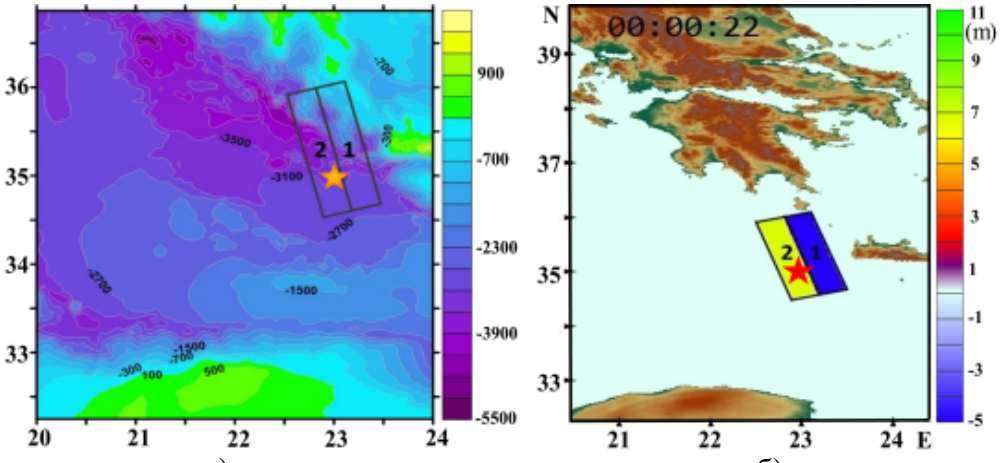

а) б)

Figure 3. Location of seismic source at earthquake of 365, SCENARIO 2
a) bathymetric map; b) topographic map.

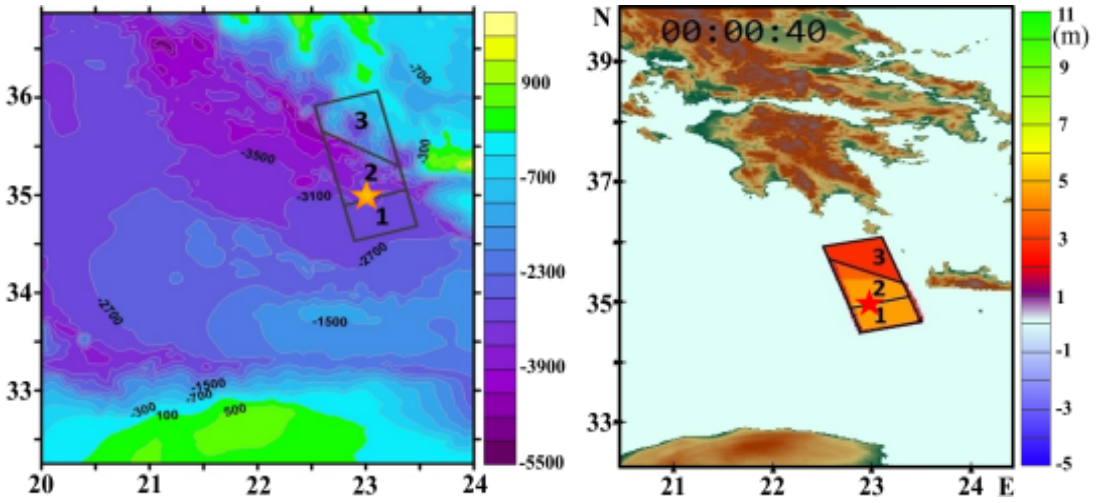

а) б)

Figure 4. Location of seismic source at earthquake of 365, SCENARIO 3
a) bathymetric map; b) topographic map.

For the second tsunamigenic earthquake of 9 February 1948, two possible scenarios of earthquake source were examined: (see Fig.5, and Fig.6)

SCENARIO 4: The seismic source being a single block which can move up and down to given values with different velocities; The block motion of this source is presented in Table 1 and the location of the seismic source is represented by Fig. 5a, b.

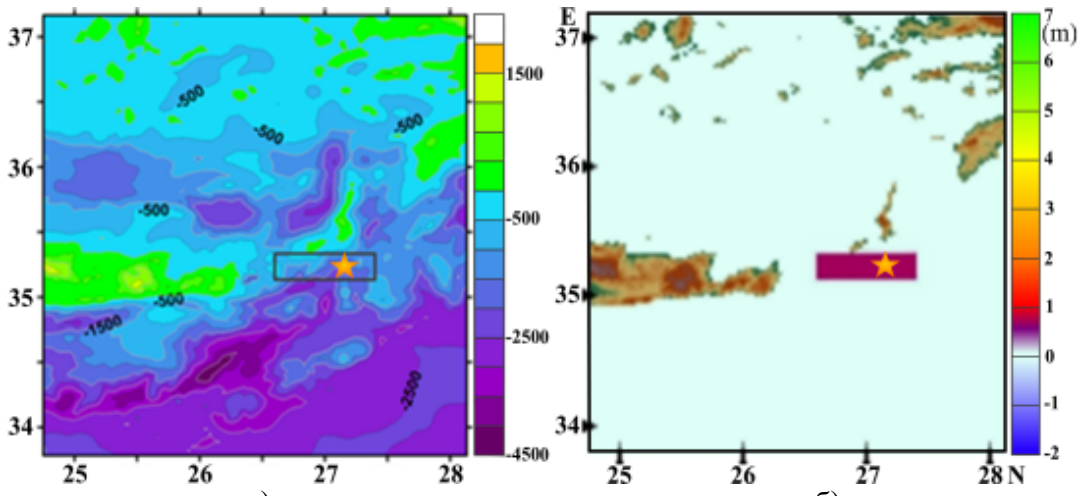

а) б)

Figure 5. Location of seismic source at earthquake of 365, SCENARIO 3
a) bathymetric map; b) topographic map.

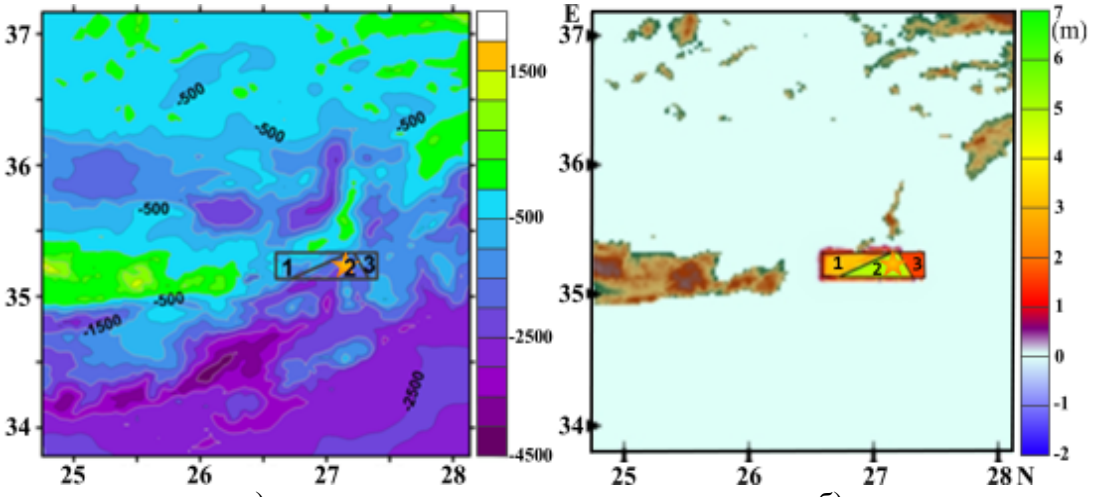

а) б)

Figure 6. Location of seismic source at earthquake of 365, SCENARIO 3
a) Bathymetric map; b) topographic map.

SCENARIO 5: For the fifth scenario the kinematics of a three-block keyboard model are considered, and the model blocks are being moved successively to different distance up and down for different length of time. The location of the seismic source for scenario 5 is presented in Fig.6a,b.

2.2. Mathematical statement of the problem

To describe the process of generation and propagation of tsunami waves in correspondence with above-mentioned assumptions, the nonlinear system of shallow water equations was used (Voltsinger et al., 1989; Lobkovsky et al., 2006)).

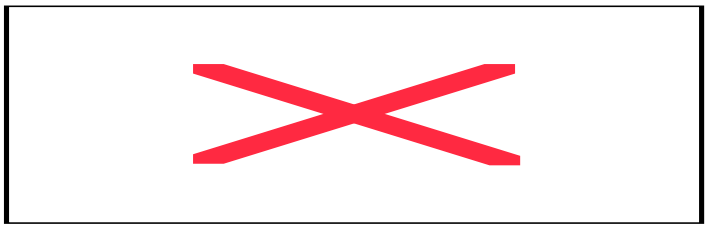

where x, y are the spatial coordinates along Ox and Oy axes, respectively, t is the time, $u(x, y, t)$, $v(x, y, t)$ are the velocity components along Ox and Oy axes, $\eta(x,y,t)$ is the disturbance of free surface relative to its initial level, H is the depth of the basin, $\phi(x, y, t)$ is the function which describes bottom motion.

3. NUMERICAL SIMULATION OF HISTORICAL TSUNAMIS

3.1. Numerical simulation of the tsunami of 21 July 365

In this section - presented as examples – are the results of implementation of SCENARIO 1 . Fig. 4, illustrates the results of numerical simulation for tsunami wave front propagation for six (6) time moments. Fig.7.1, shows that the initial tsunami wave front already has reached points on Falaserna and Palaiochora at the west coast of the Island of Crete and the nearby islands. At 23 minutes travel time the initial wave front reaches the south side of the coast of Glyfada, on Attica , Greece(Fig.7.2).

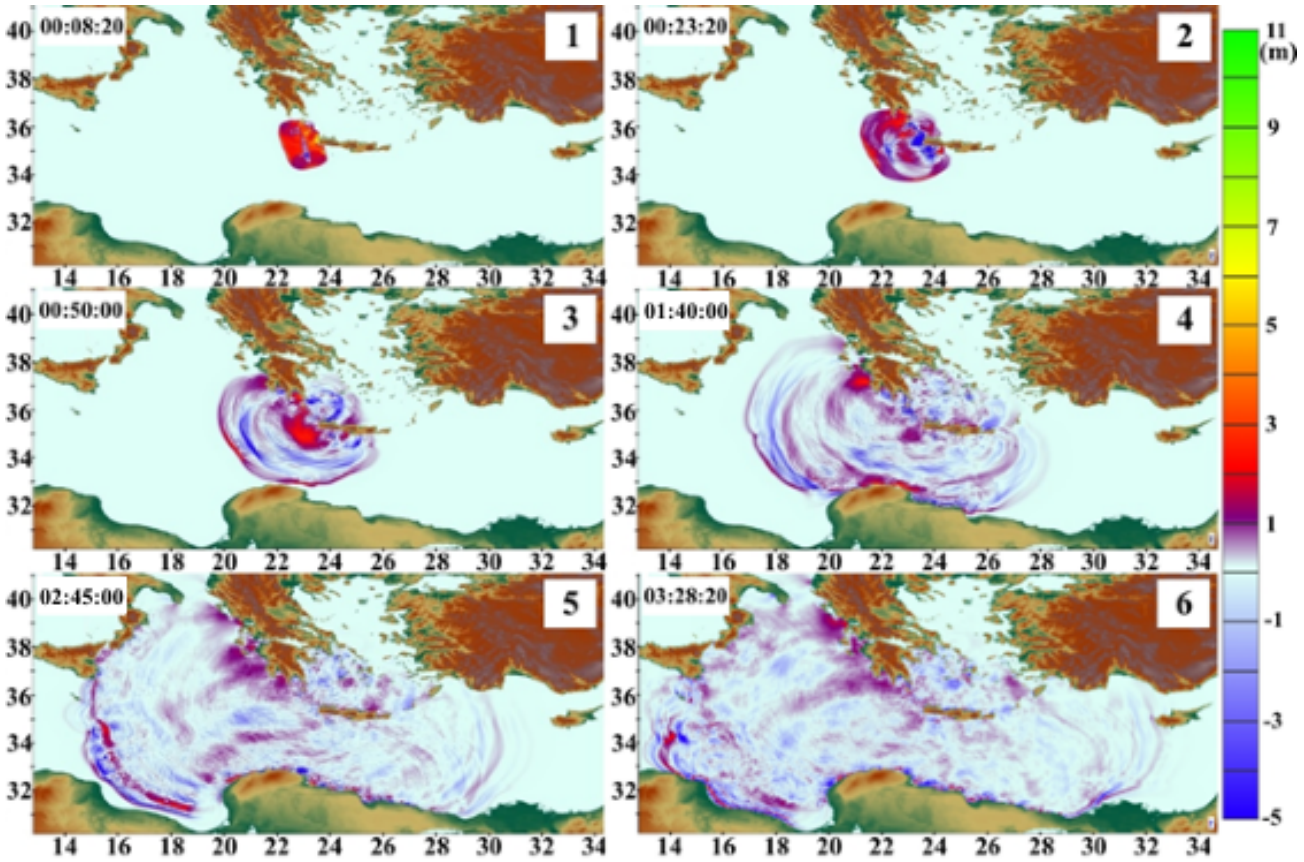

Figure 7. Propagation of the tsunami wave for scenario 1 for six time increments: 1 - 8 min 20 s; 2 - 23 min 20 s; 3 - 50 min; 4 - 1h 40 min; 5 - 2 h 45 min; 6 - 4h 30 min.

At the 50th minutes the first tsunami wave front reaches the African continent in the region of Point Derna of the coast of Libya (Fig.7.3). Further propagation of the tsunami wave front (for 1 h 40 min), strikes another Libyan coastal region of Benghazi and Turku cities, as well as the region of Katakola and Kalamata cities on the coast of Greece (Fig.7.4). After 2 h 45 min (Fig.7.5) the forefront of tsunami has already struck all three continents as well as the coast of Catania on the Island of Sicily (Fig.7.6).

Shown in Fig.8 are the computed distributions of maximum tsunami wave heights in the Eastern Mediterranen basin. As seen, the maximum wave heights occurred along the Greek coasts (maximum heights near the Island of Crete), the coasts of Italy, and near the northern and north-western coast of the African continent.

In more detail, the distribution of maximum wave heights along the coasts can be seen at the 3D-histograms of maximum wave heights, at the 5-m isobath (Fig.9). It can be seen that the coasts of Italy and the Island of Crete the wave heights reached 5-8 m. At the Island of Cyprus the mean wave heights were 2 m with 5 m peaks at some segments.

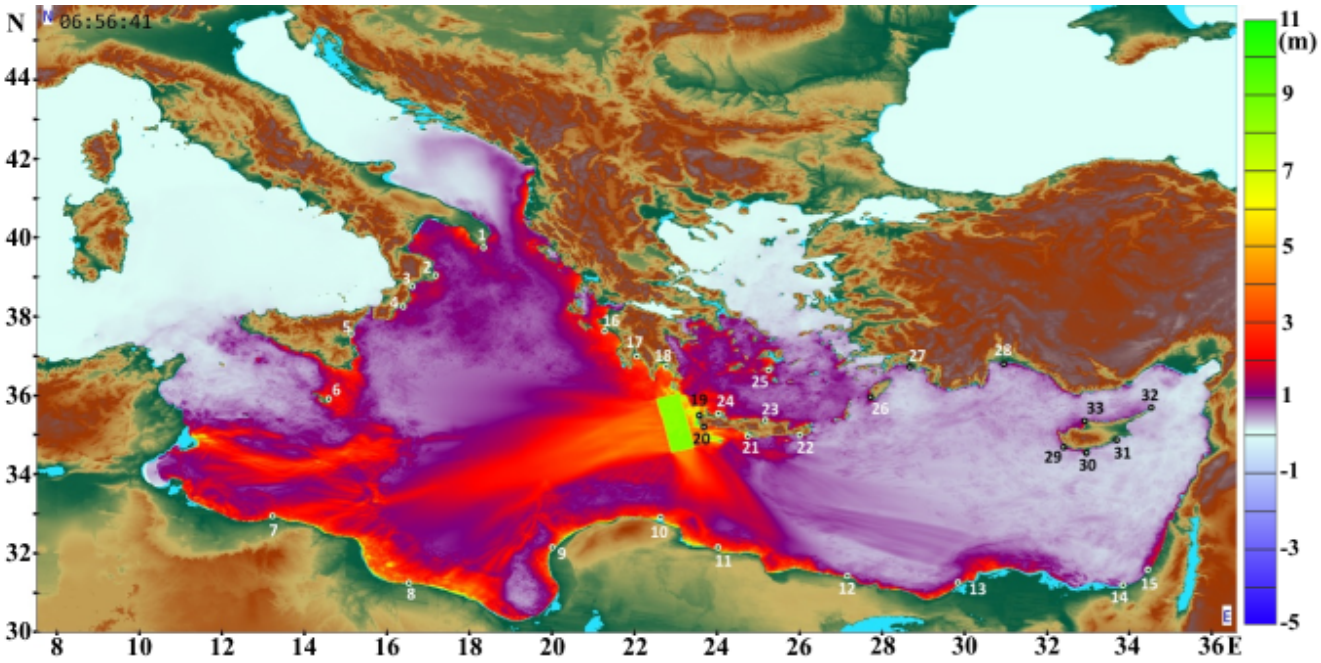

Figure 8. Distribution of maximum wave heights over the basin with implementation of scenario 1.

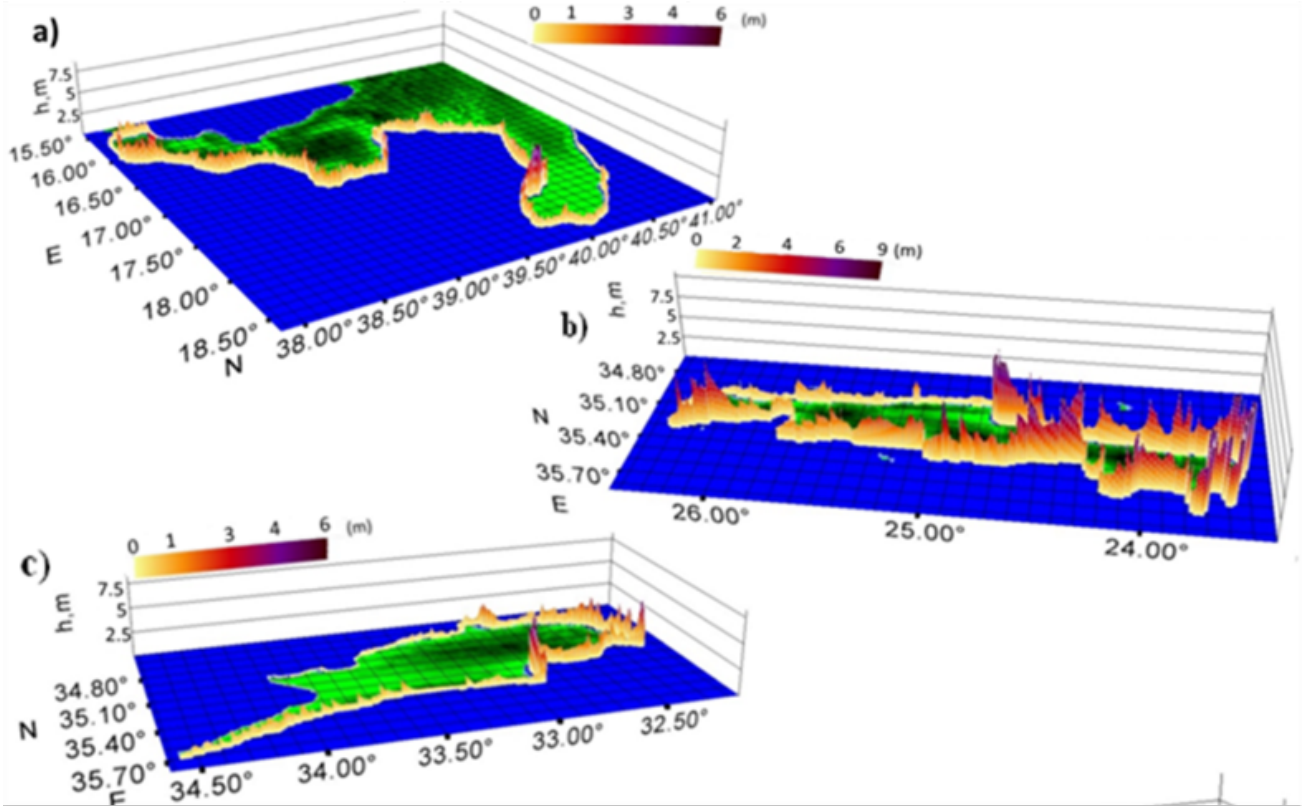

Figure.9. 3D-histograms for maximum wave heights at the 5-m isobath: a) Italy; b) Island of Crete; c) Island of Cyprus.

3.2. Results of the numerical simulation for scenario 3

For the realization of scenario 3 the keyboard model of seismic source is the same as for scenario 1 (Fig.4). Fig.10 illustrates tsunami wave generation for three (3) time increments and the location of the tsunami wave front for five (5) time icrements. The first 3 figures (Fig.10 (1-3)) illustrate this after tsunami generation.

Fig.10 (5) shows that the elevation of the wave coming to the Island of Crete and its directivity towards southern Greece. Figure 10 (6) shows the northern front striking the southern coast of Greece and heading for the City of Katakolo. The 50th minute wave has struck one half of the Island of Crete and other parts of Greece while the southern front of the wave is coming to Derna City. Subsequently the tsuanmi wave front is seen to propagate towards the coasts of the African continent. In three (3) hours the wave front is seen to have reached Sirt City in Libya, while the north-west front of the tsunami reaches the eastern coast of Italy, the north-east front begins to reach the coast of Turkey and finally the southern-eastern front of the wave begins to strike the City of Alexandria.

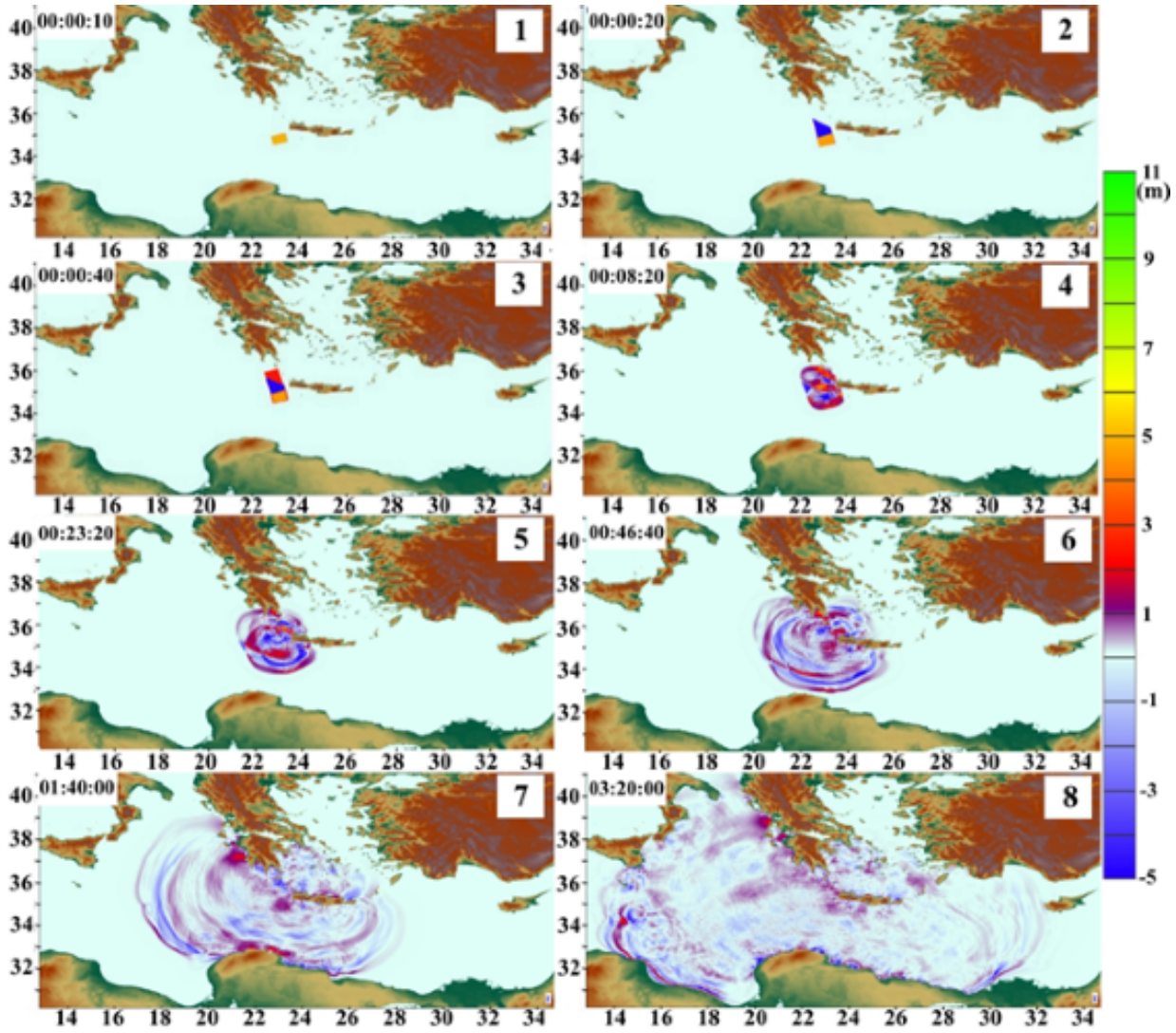

Figure 10. Numerical simulation of scenario 3: a) generation of tsunami source: 1) 10 sec, 2) 20 sec, 3) 40 sec; b) wave front localization: 4) 8 min 20 sec; 5) 23 min 20 sec; 6) 46 min 40 sec; 7) 1 hour 40 min; 8) 3 hours 20 min;

Fig.11 illustrates the computed distributions of maximum wave heights within the Eastern Mediteranean basin for the given scenarios. As seen the wave heights' distribution is close to the wave heights of the first and second scenarios but differently-oriented motion of blocks at the source significantly decreases wave height at the coast of Sicily coast and increases the height of waves at the coasts of Turkey. The more dangerous sections of tsunami wave heights concentrates mainly along the remains to be the coasts of Tunisia, Libya, Italy, Greece, Turkey, Egypt, Crete and Malta.

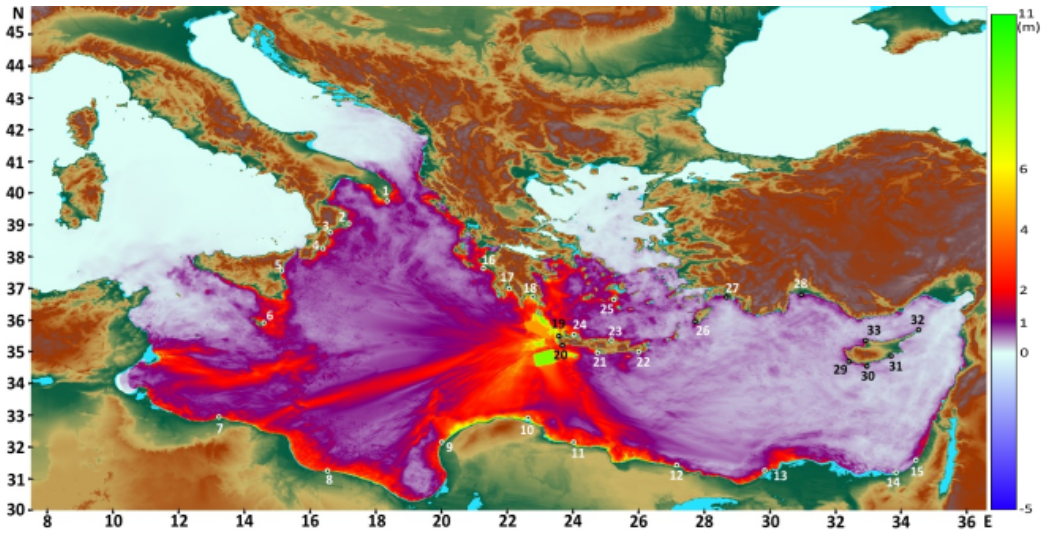

Figure 11. Maximum tsunami wave heights in Eastern Mediterranean basin for scenario 3.

Presented in Fig.12 are 3D histograms for the coasts of Libya, Tunisia and the eastern coasts of Mediterranean Sea: Israel, Lebanon, Syria. Apparently the wave height at eastern coast of Mediterranean Sea reached 4 m, and the at coasts of Libya and Tunisia up to 7m.

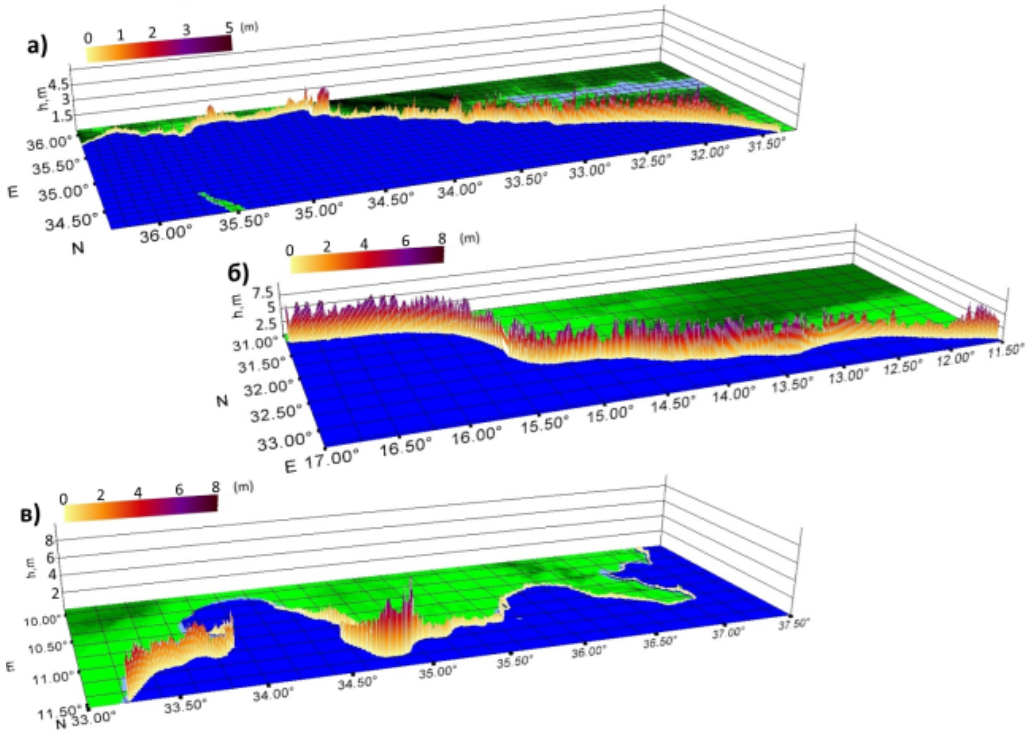

Figure 12. 3D histogram for maximum tsunami wave at 5 m isobath: a) eastern coast; b) Libya; c) Tunisia.

3.3. Numerical simulation of the tsunami of 9 February 1948

The results of implementation of SCENARIO 5 are presented in this section. It is well known that processes occurring at a seismic source (uplift or downfall), can be ultimately recalculated to estimates of vertical displacements. Presented in Fig.13 is an illustration of tsunami generation by displacements along a three-block seismic source. The process of formation of tsunami source can be seen with the uplift of the first crustal block on the seafloor, then at the downward motion of a second block and then by the subsequent uplift of a third block to the same height as the first.

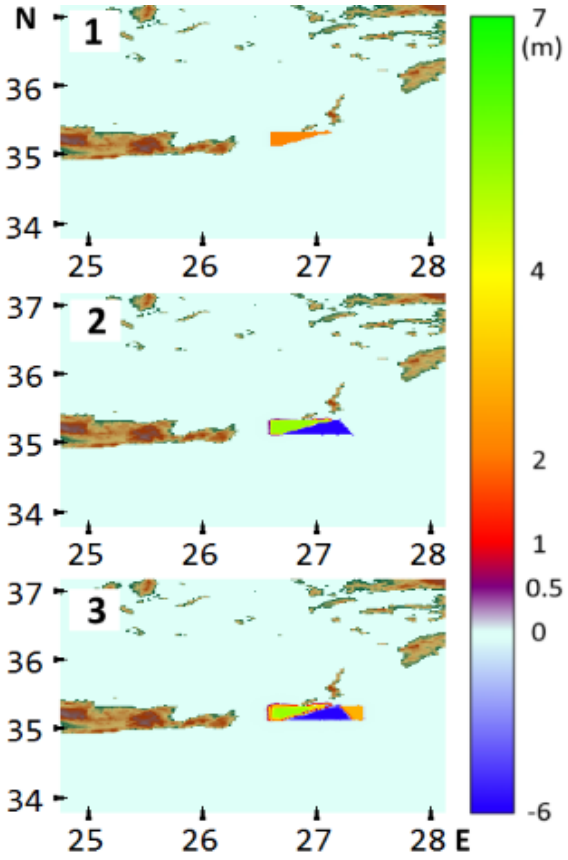

Figure 13. Generation of tsunami source with the realization of scenario 5: 1) 5 s; 2) 14 s; 3) 25 s.

Illustrated by Fig.14, is the propagation of tsunami waves on the basin for six (6) time icrements. In the first time increment (Fig.14 (1), the wave is seen to strike the Island of Karpathos as well as the western coast of the Island of Crete. Subsequently, in 21 min (Fig.14 (2)), the leading tsunami wave reaches the Greek Island of Rhodes. At further propagation (55 min, middle panel, Fig.14 (3)) the wave's north-eastern front has already reached the Island of Rhodes and stikes the south-eastern cities of Dalyan and Marmaris inTurkey.

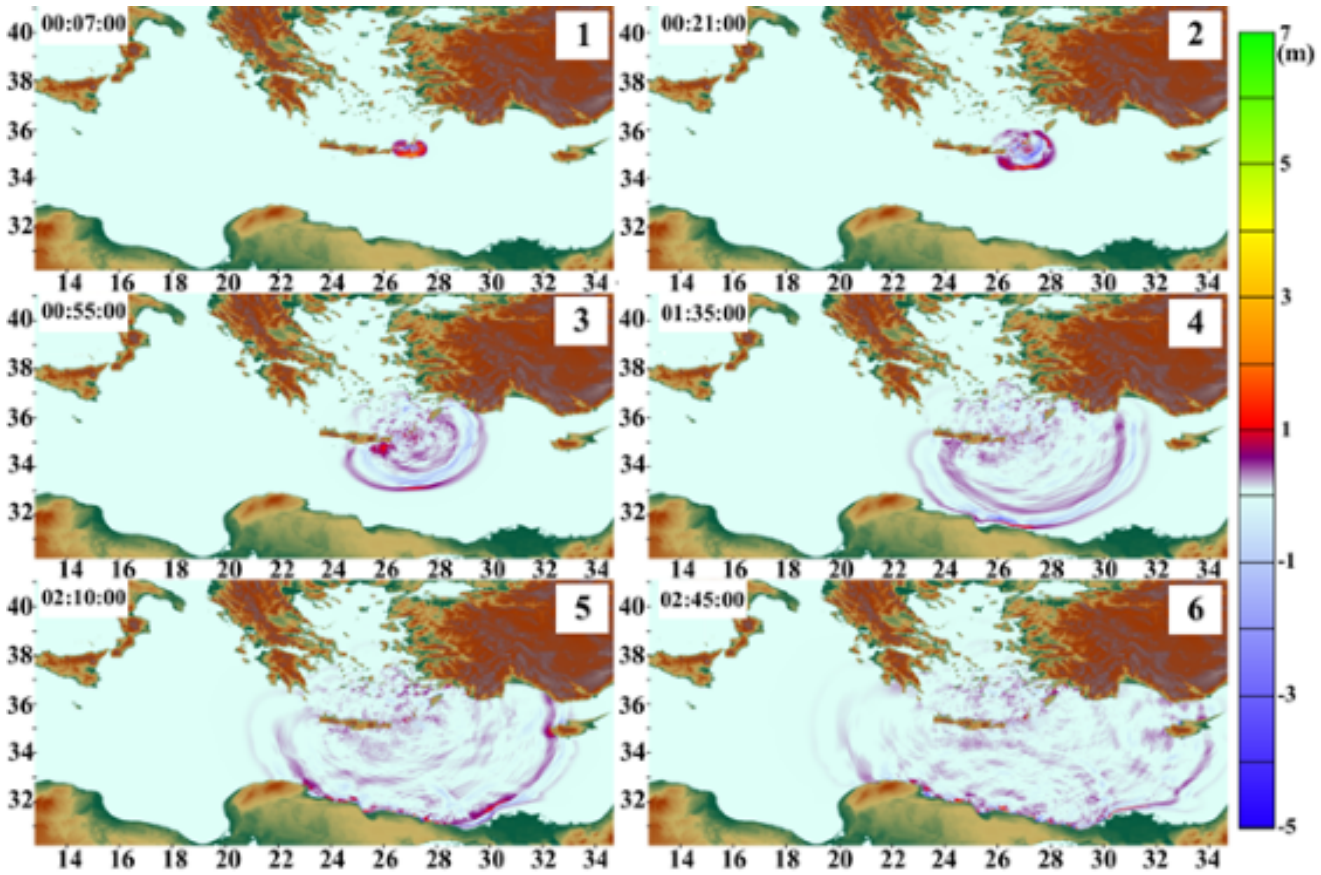

Figure 14. Numerical simulation of scenario 4: a) generation of tsunami source: 1) 7 sec, 2) 21 sec, 3) 55 min, 4) 1 hour 35 min, 5) 2 hour 10 min, 6) 2 hour 45 min.

In 1 hour and 35 min (middle panel, Fig.14 (4)), the wave has already reached the Island of Crete, its southern front has already reached the coast of Mersa-Matruh and begins to arrive at the east of Libya. In 2 hour and 10 min (lower panel, Fig.14 (5)) the eastern front actively strikes part of the Island of Crete and the southern coast of Turkey in the region of Alanya City. At the lower panel, (2 hour 45 min, Fig.14 (6)) the southern front has already reached a large part of the coast of Egypt, while the north-western front has reached the south coasts of Greece.

Presented in Fig.15, is the distribution of maximum wave heights in the entire basin of the Eastern Mediterranean Sea. From the distribution of maximum wave heights for the fifth scenario it is well seen that most affected are the near-field segments of the coasts of Libya, Egypt, Turkey, and of the Islands of Crete and Cyprus.

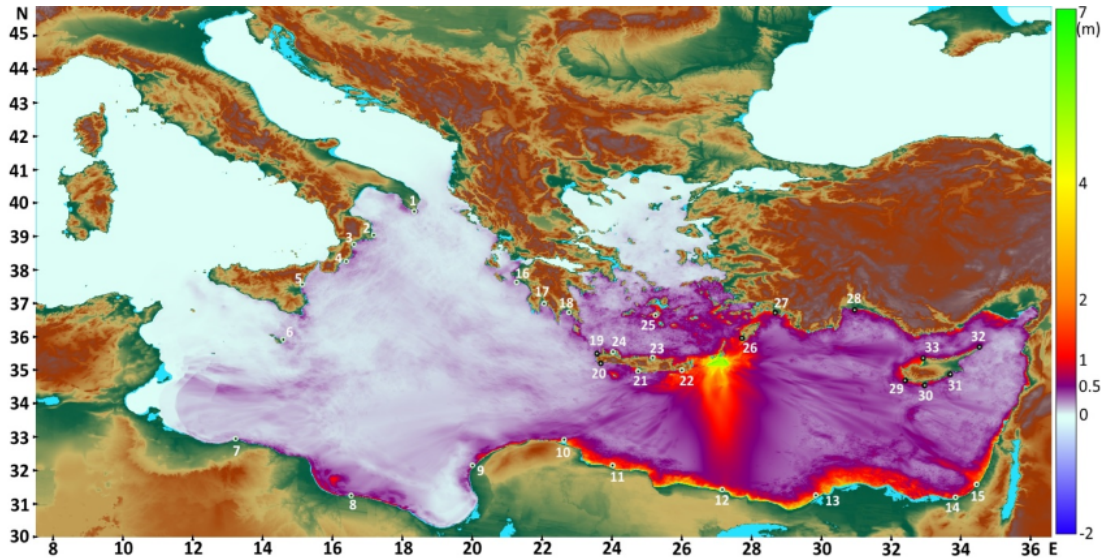

Figure 15. Maximum tsunami wave heights on the Eastern Mediterranean basin at the realization of scenario 5.

Fig.16 shows the 3D-histograms for maximal wave heights at 5-m isobath for the coasts of Turkey, the Island of Crete, and Israel, Lebanon and Syria.

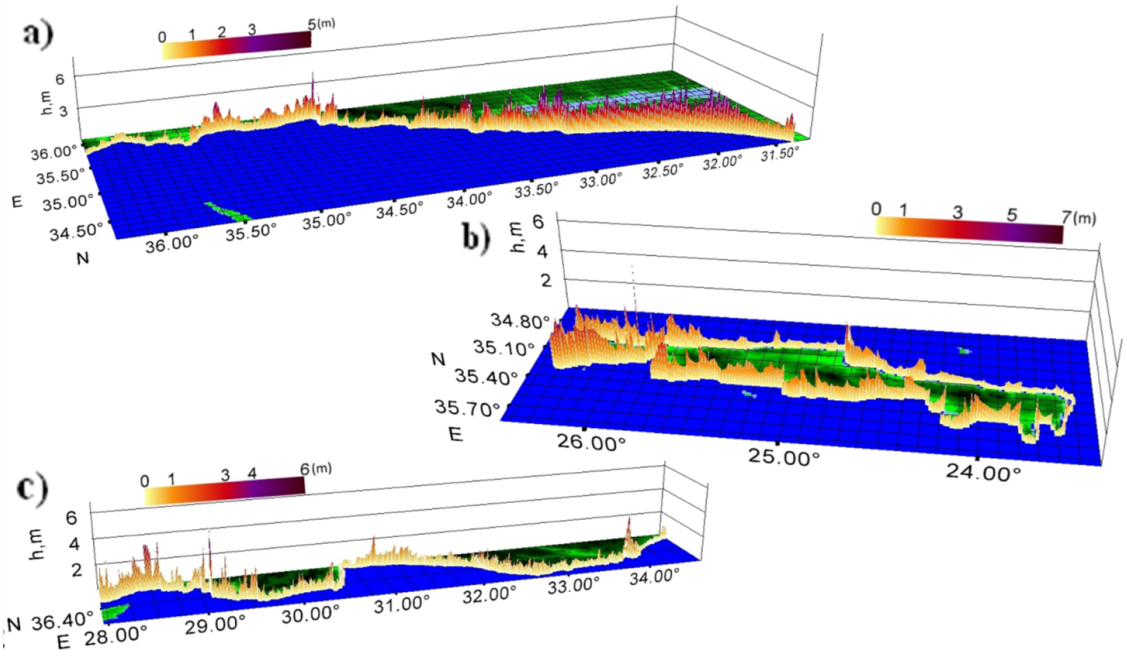

Figure 16. 3D-histograms for maximum wave heights at 5-m isobath for the coasts of: a) theeast coast of Mediterranean Sea; b) Crete island; c) Turkey.

4. COMPARISON OF MAXIMUM WAVE HEIGHTS FOR EARTHQUAKE AND TSUNAMI OF 21 JULY 365 AND 9 FEBRUARY 1948

4.1. Comparison of maximum wave heights for earthquake and tsunami of 21 July 365

Fig.17 shows histograms of maximum wave heights for the coast of the Island of Crete. As it can be seen, at the west of the southern coast, the maximum wave height of 7.6 m is reached with the first and second (single block and two-block source, respectively) scenarios. For the third scenario (three-

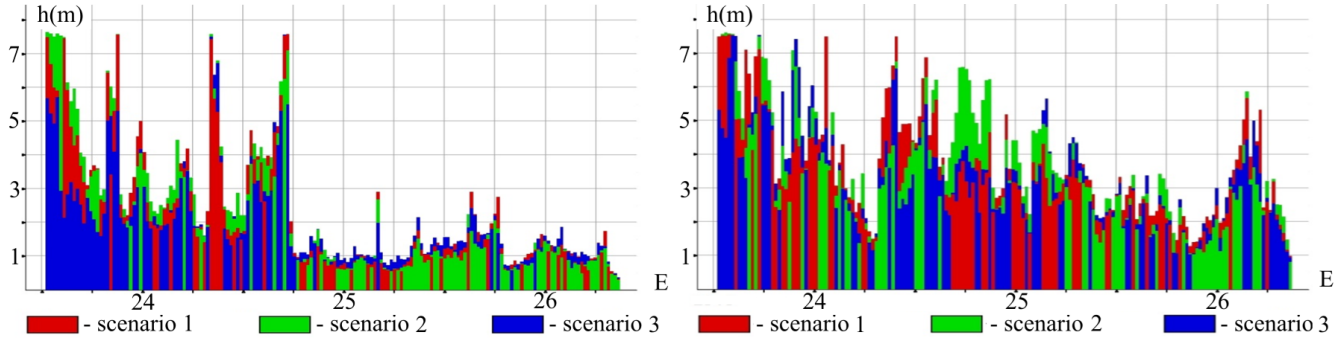

Figure 17. Histograms of maximum tsunami wave heights for the Island of Crete: a) southern coast; b) eastern coast.

block source) the maximum wave height is 6.5 m, while mean values of the tsunami wave height are near 2.8 m. Fig.18 illustrates histograms for the coast of Sicily. It can be seen that maximum tsunami wave heights to 5.5 m are reached with the realization of scenario 2. However, at the eastern coast of the Island of Sicily, the maximum wave height to 6.5 m is reached with the realization of scenario 3.

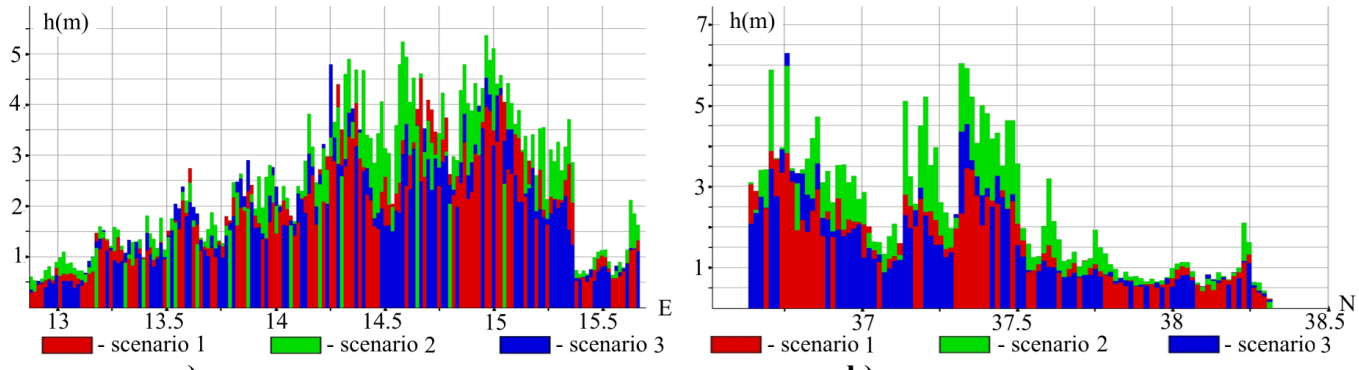

Figure 18. Histograms of maximum tsunami wave heights for the Island of Sicily: a) south-eastern coast; b) eastern coast.

Fig.19a shows a histogram of maximum wave heights for the Turkish coast. It is well seen that with the realization of all scenarios, the maximum wave heights in the the west reaches 2,75 m but at eastern side the maximum wave heights are reached with the realization of scenario 1.

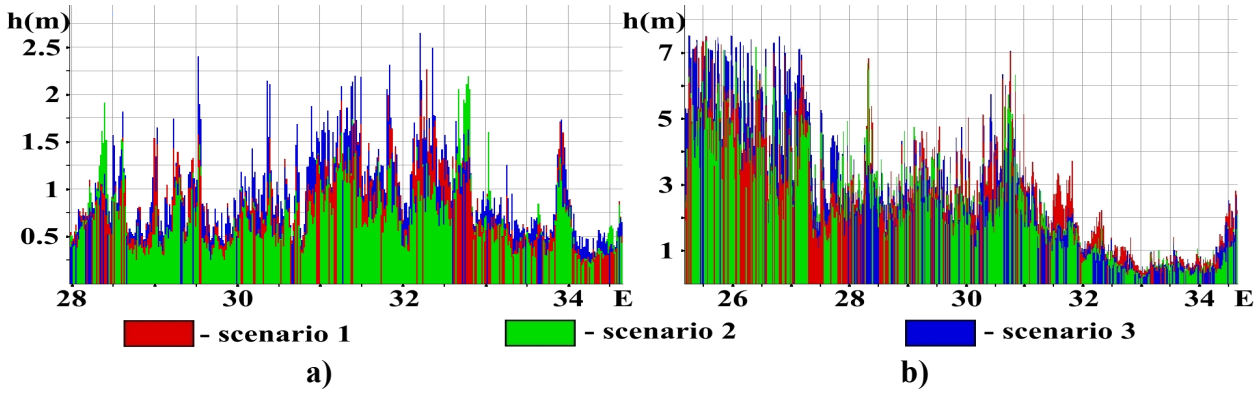

Figure 19. Histograms of maximum tsunami wave heights for the Turkish coast (a) and for the coast of Egypt (b).

Fig.19b ahows the histograms of maximum wave heights on the coast of Egypt. It can be seen that the maximum wave height of 7.2 m is reached with the realization of scenario 3.Table 5 shows the data from virtual tide gauges, namely maximum wave height, as well a depression of water level and time of arrival for scenarios 1-3.

4.2. Comparison of maximum wave heights for earthquake and tsunami 9 February 1948

Fig. 20 shows the histograms of maximum tsunami wave heights for the coast of Italy for cases when seismic source is a single block (scenario 4) and for a three-block keyboard source (scenario 5). Maximum wave heights for both scenarios are reached to 0.6 m.

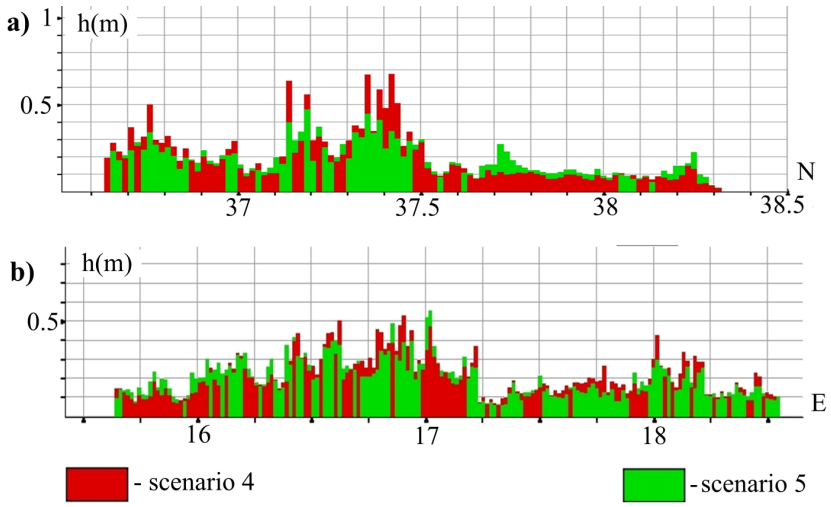

Figure 20. Histograms of maximum tsunami wave heights for the coast of Italy coast: a) eastern coast; b) southern coast.

Fig. 21 shows the histograms of maximum tsunami wave heights for the coast of the Island of Crete. A maximum wave height of 4 m is reached with the realization of scenario 4. For scenario 5 the maximum wave height id 3.5 m.

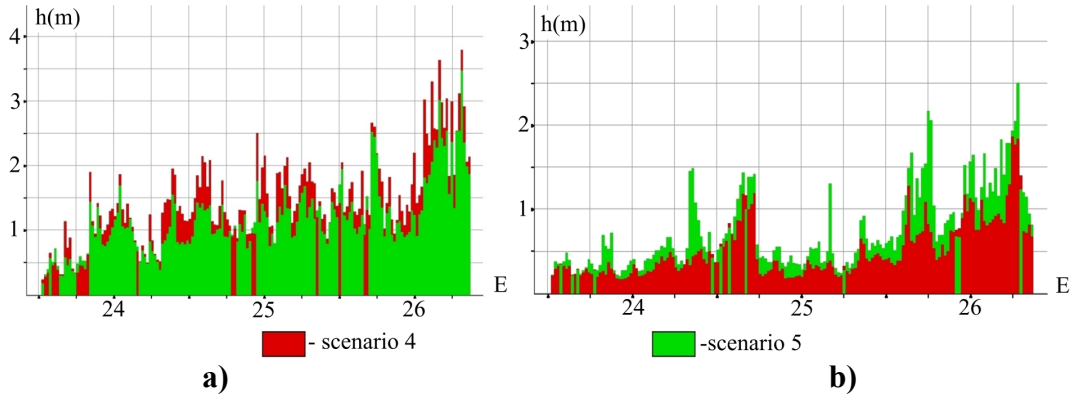

a) **b)**

Figure 21. Histograms of maximum tsunami wave heights for the Island of Crete: a) southern coast; b) eastern coast.

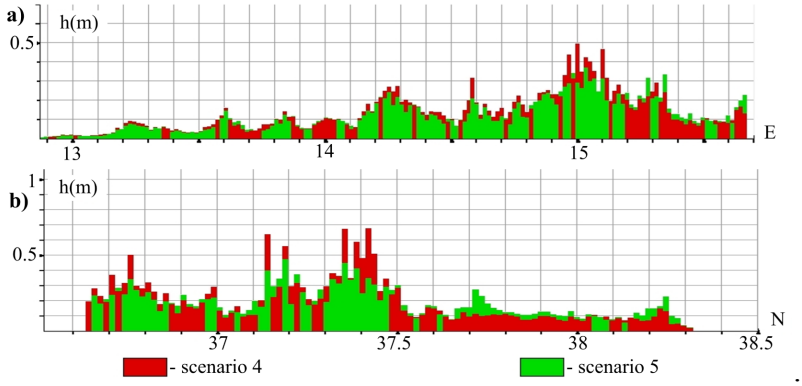

Figure 22. Histograms of maximum tsunami wave heights for the Island of Sicily: a) southern coast; b) eastern coast.

Fig. 22a shows the histograms of maximum wave heights for the southern coast of the Island of Sicily for two scenarios. Maximum wave height for both scenarios reaches 0.5 m. Fig. 22b shows histograms of maximum wave heights for the eastern coast of Sicily. A maximum wave height of 0.7 m is reached with the realization of scenario 4. However, the mean wave height near the coast for both scenarios is not essentially different.

Fig. 23a shows histograms of maximum wave heights for the coast of Turkey. Maximum wave height reaches 3.8 m, however, the mean values along the coast do not exceed 1.5 m. Fig. 23b is a histogram of maximum tsunami wave height for the coast of Egypt. It is well seen that with the realization of scenario 4 the wave heights reach 10 m while for scenario 5 their heights range between 5 and 8 m. With the realization of scenario 4, the mean wave height is essentially larger than with the realization of scenario 5.

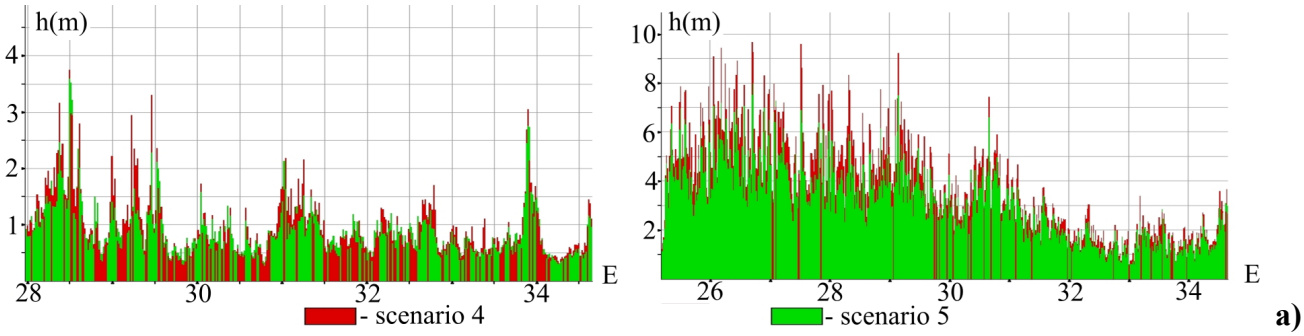

Figure 23. Histograms of maximum tsunami wave heights for the Turkish coast (a) and for the coast of Egypt (b).

The numerical simulation and analysis of maximum wave heights of the historical tsunamis of 345A.D. and 1948 A.D. for selected 33 points of the Eastern Mediterranean basin, with the given earthquake magnitude but with different realization of initial conditions (see Tables 1 and 2), gives far-field values independently of the dynamics of the seismic source. But for the near-field zones the values essentially depend on the crustal displacement processes at the source of the earthquake.

Table 1. shows the data of maximum high and low values of 33 virtual tide gauges (see Figures 8,11,15) at the 5-meter isobath, for SCENARIOS 1-5.

Table 1

№	Settlement/inhabited locality	Maximum ampltitudes at the 5-meter isobath (m)					The largest decrease in the water level of 5-meter isobath (m)				
		Scenario №									
		1	2	3	4	5	1	2	3	4	5
1	c. Leuca	3,79	3,67	2,57	0,18	0,19	3,55	3,52	3,01	0,11	0,11
2	c. Crotone	3,33	3,90	2,40	0,15	0,14	3,21	3,85	2,59	0,18	0,15
3	c.Catandzaro	2,21	2,19	1,59	0,09	0,11	1,90	1,85	1,44	0,12	0,11
4	c.RoccellaIonica	3,27	4,29	2,74	0,88	0,48	4,09	4,17	3,15	0,69	0,58
5	c. Catania	2,32	4,62	1,87	0,34	0,29	3,50	4,10	3,12	0,20	0,26
6	c. Valletta	3,46	4,13	2,22	0,11	0,11	3,05	3,97	2,72	0,14	0,13
7	c. Tripoli	3,26	4,95	3,18	0,13	0,09	4,30	5,59	3,92	0,14	0,13
8	c. Sirt	4,27	4,62	4,82	0,27	0,25	3,75	6,77	3,28	0,26	0,21
9	c. Benghazi	3,64	5,19	2,71	1,19	1,06	3,17	3,45	2,78	1,16	0,92
10	c. Derna	4,32	5,10	4,04	0,65	0,69	5,09	5,71	3,98	0,65	0,51
11	c. Tobruk	5,07	3,21	4,56	1,44	1,29	3,69	3,07	3,47	1,72	1,55
12	s. MersaMatruh	3,02	3,93	3,27	5,77	5,25	2,66	2,93	2,78	3,69	3,62
13	c. Alexandria	2,43	2,27	1,92	1,97	1,90	2,82	2,82	2,44	1,80	1,74
14	c. Al-Arish	0,72	0,58	0,73	0,79	0,88	0,70	0,46	0,62	1,08	0,93

15	**c. Gaza**	**1,27**	**1,23**	**1,18**	**1,11**	**1,00**	**1,06**	**1,15**	**0,98**	**1,15**	**0,83**
16	**c. Katakolo**	**3,62**	**3,45**	**3,76**	**0,33**	**0,30**	**4,02**	**3,75**	**3,59**	**0,41**	**0,30**
17	**c. Kalamata**	**6,49**	**5,68**	**3,96**	**0,66**	**0,36**	**6,93**	**4,98**	**5,27**	**0,73**	**0,57**
18	**c. Glyfada**	**6,85**	**6,38**	**6,82**	**0,46**	**0,42**	**6,52**	**6,82**	**8,49**	**0,54**	**0,47**
19	**c. Phalasarna**	**6,94**	**6,09**	**6,99**	**0,29**	**0,28**	**6,98**	**7,96**	**6,56**	**0,31**	**0,29**
20	**c. Palaiochora**	**6,98**	**6,69**	**6,74**	**0,61**	**0,50**	**5,84**	**6,23**	**5,90**	**0,49**	**0,42**
21	**v. Matala**	**5,62**	**5,06**	**6,98**	**1,21**	**1,35**	**6,17**	**5,38**	**5,40**	**1,52**	**1,54**
22	**c. MakryGialos**	**6,66**	**6,40**	**7,08**	**1,80**	**1,57**	**3,94**	**5,15**	**3,23**	**1,58**	**1,34**
23	**c. Heraklion**	**3,58**	**3,07**	**2,82**	**0,82**	**0,81**	**2,29**	**3,15**	**2,15**	**0,81**	**0,74**
24	**c. Chania**	**4,32**	**4,08**	**3,62**	**1,12**	**0,73**	**4,52**	**9,42**	**4,07**	**1,33**	**1,01**
25	**i. Ios**	**2,61**	**2,67**	**2,58**	**0,81**	**0,65**	**2,79**	**2,85**	**3,09**	**0,80**	**0,58**
26	**c. Prasonisi**	**3,16**	**2,81**	**2,34**	**3,16**	**2,87**	**3,01**	**3,52**	**1,92**	**2,71**	**2,59**
27	**b.Iztuzu**	**2,75**	**3,61**	**3,09**	**2,00**	**1,82**	**3,73**	**4,34**	**4,69**	**2,74**	**2,53**
28	**c. Belek**	**2,02**	**3,78**	**3,80**	**2,64**	**2,09**	**2,70**	**3,47**	**5,50**	**2,47**	**2,07**
29	**c.Paphos**	**2,53**	**1,46**	**2,08**	**1,30**	**1,09**	**2,36**	**2,07**	**2,01**	**1,14**	**1,17**
30	**b. Akrotiri**	**2,47**	**1,91**	**2,70**	**1,89**	**1,62**	**1,38**	**2,25**	**2,18**	**1,56**	**1,22**
31	**c. Larnaca**	**0,65**	**0,38**	**0,54**	**0,35**	**0,33**	**0,62**	**0,41**	**0,48**	**0,35**	**0,34**
32	**p.Karpass**	**0,37**	**0,29**	**0,32**	**0,21**	**0,23**	**0,52**	**0,39**	**0,45**	**0,24**	**0,18**
33	**v. Livera**	**2,21**	**2,90**	**1,91**	**2,10**	**1,49**	**1,94**	**4,03**	**1,92**	**2,31**	**1,37**

5. DISCUSSION AND CONCLUSION

The above obtained results for potential tsunami waves generated by great earthquakes in the Mediterranean Sea, demonstrate that detailed tsunami characteristics can be essentially determined by location of seismic source and analyzing the complexity of crustal displacement processes. Use of the key-board model for such tsunamigenic earthquakes permits to take into account such complexities. The present data on generation and propagation of tsunami waves at realization of the three listed scenarios are consistent with the results of numerical simulation of the 365 A.D. event with another model of the seismic source (Pararas-Carayannis, Mader, 2011). So, as it follows from both models the western part of Mediterranean Sea is not affected (Pelinovsky et al., 2002)) while in the Eastern Mediterranean larger tsunamis can be expected. The somewhat higher wave heights in the deeper sea region in the model by Pararas-Carayannis and Mader (2011) can be the result of higher initial vertical displacement at the seismic source (~ 50m) as compared with the gradual value of our computation. Fig. 24a, shows a histogram of results of computation of maximum wave heights using the key-board model for the great tsunamigenic earthquake of 21 July 365 A.D.. Though the general character of the histogram is consistent with that computed for the standard model of seismic source (Fig. 24b), the distribution of tsunami wave heights is somewhat different. In addition, from Fig. 24a it is well seen that maximum wave heights can exceed 5 m, while wave heights in histogram from work [11] are somewhat less.

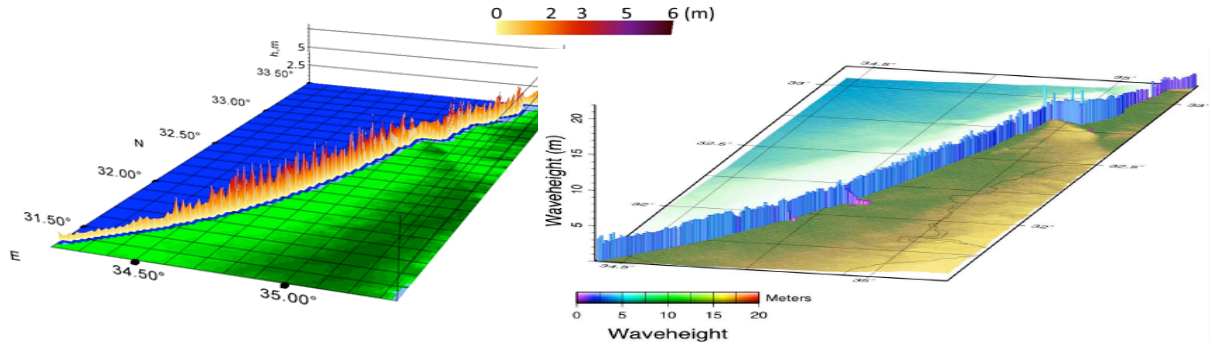

a) **b)**

Figure 24. Comparison of histograms of distribution of maximum wave heights for great earthquake of 21 July 1948 A.D. at the east coast of the Mediterranean Sea: a) present results; b) data from work [11].

So, numerical simulation performed to model historic tsunami in Mediterranean Sea, generated by great earthquakes occurred in 21 July 365 and 9 February 1948, demonstrates that for large and great earthquake, tsunami wave heights in some points of Mediterranean Sea's coast can reach 9 m. Such result relates mainly to near-field tsunami. It is necessary to note that depending on geodynamics of earthquake source, scatter of maximum heights at the coast under the same earthquake magnitude can differ in to 1.5-2 times. For far-field tsunami maximum wave heights can exceed 5 m.

ACKNOWLEDGEMENTS

This work was supported by the Russian Science Foundation, project no. 14-50-00095.

REFERENCES

EC (Earthquakes on Crete), 2016: http://www.sfakia-crete.com/sfakia-crete/earthquake.html

Lobkovsky L.I., 1988. Geodynamics of zones of spreading, subduction and two-level plate tectonics (Nauka Press, Moscow, USSR, 1988).

Lobkovsky L.I., Mazova R.Kh., Kataeva L.Yu., Baranov B.V., 2006. Generation and propagation of catastrophic tsunami in the basin of Sea of Okhotsk. Possible scenarios", Doklady 410, 528-531.

Mazova R., Tyuntyaev S., 2016. Tsunami at Sicilian coast from numerical simulation of two historical Mediterranean earthquakes, Abst.Book of 15th Plinius Conf. on Mediterranean Risks, 17.

Papadopoulos P., Daskalaki E., Fokaefs A., Giraleas N., 2010. Tsunami hazard in the Eastern Mediterranean Sea: Strong earthquakes and tsunamis in the west Hellenic arc and trench system, J. of Earthq. and Tsunami 4, 145-151.

Papazachos, B. C. 1996. Large seismic faults in the Hellenic arc. Ann. Geofis. 39, 891–903.

Pararas-Carayannis, G., 2001. The Potential for Tsunami Generation in the Eastern Mediterranean Basin and in the Aegean and Ionian Seas in Greece.
http://www.drgeorgepc.com/TsunamiPotentialGreece.html

Pararas-Carayannis, G., 2006. The Earthquake of January 8, 2006 in Southern Greece.
http://www.drgeorgepc.com/Earthquake2006Greece.html

Pararas-Carayannis G., Mader C.L., 2011. The Earthquake and Tsunami of 365 A.D. in the Eastern Mediterranean, Sci. of Tsunami Hazards, 30 (4), 1-10.

Pelinovsky E., Kharif C., Riabov I., Francius M. 2002. Modelling of Tsunami Propagation in the Vicinity of the French Coast of the Mediterranean, Natural Hazards 25, 135–159.

Salamon A., Rockwell T., Ward S.N., Guidoboni E., Comastri A., 2007. Tsunami Hazard Evaluation of the Eastern Mediterranean: Historical Analysis and Selected Modeling, Bull.Seism.Soc.Am., 97, 1–20. doi: 10.1785/0120060147.

Shaw B., Ambraseys N.N., England P.C., Floyd M.A., Gorman G.J., Higham T.F.G., Jackson J.A., Nocquet J.-M., Pain C.C., Piggott M.D., 2008. Eastern Mediterranean tectonics and tsunami hazard inferred from the AD 365 earthquake, Nature Geosci. 1, 268-276.

Sielecki A., Wurtele M., 1970. The numerical integration of the non-linear shallow-water equations with sloping boundaries, J.of Comp. Phys., 6, 219-236.

Thio H.K., 2009. Tsunami hazard in Israel, in: Report of URS Corp, Pasadena, USA, 2009, 72.

Tinti S., Armigliato A., Pagnoni G., and Zaniboni F., 2005**.** Scenarios of giant tsunamis of tectonic origin in the Mediterranean, ISET J. of Earthq. Techn., 42, 171-188.

Voltsinger N.E., Klevanny K.A., Pelinovsky E.N., 1989. Long-Wave Dynamics of Coastal Zone, (Gidrometeoizdat, Leningrad, USSR, 1989).

Wells D.L., Coppersmith K.J., 1994. New empirical relationships among magnitude, rupture length, rupture width, rupture area, and surface displacement, Bull.of Seism.Soc.of Am., 84. 974-1002.

Yolsal-Çevikbilen S., Taymaz T., 2012. Earthquake source parameters along the Hellenic subduction zone and numerical simulations of historical tsunamis in the Eastern Mediterranean, Tectonophysics,. 536–537, 61-63.